Synchronization of Frequency Modulated Multi-Agent Systems

Zhiyong Chen

***Abstract*—Oscillation synchronization is a widely observed phenomenon in natural systems through frequency modulated signals, especially in biological neural networks. Frequency modulation is also one of the most widely used technologies in engineering. However, due to technical difficulties, oscillations have always been simplified as unmodulated sinusoidal-like waves in studying the synchronization mechanism in the bulky literature. The application of mathematical principles, especially systems and control theories, is lacking for frequency modulated multi-agent systems. This paper aims to introduce a new formulation of the synchronization of frequency modulated multi-agent systems. It develops new tools to solve the synchronization problem by addressing three issues: frequency observation in nonlinear frequency modulated oscillators subject to network influence, frequency consensus via network interaction subject to observation error, and a well-placed small-gain condition among them. The architecture of the paper consists of a novel problem formulation, rigorous theoretical development, and numerical verification.**

***Index Terms*—Multi-agent systems, oscillators, synchronization, frequency modulation, networked systems**

I. Introduction

Frequency modulated signals exist extensively in natural network systems, such as neural circuits. Neuroscientists are interested in modeling nervous systems from simple neural networks to the human brain. One of the basic areas is the study of the neural network models for rhythmic body movements during animal locomotion. Such spinal neural networks are called central pattern generators (CPGs), which, as oscillator circuits, can generate coordinated signals for rhythmic body movements. It has been well understood that *"most neurons use action potentials (APs), brief and uniform pulses of electrical activity, to transmit information... the strength at which an innervated muscle is flexed depends solely on the 'firing rate,' the average number of APs per unit time (a 'rate code')"* [1]. In other words, the transmitted signals are frequency modulated. For example, the frequency modulated signals recorded in a real CPG network are shown in Fig. 1 for the dorsal-ventral swimmer *Tritonia*, a genus of sea slugs.

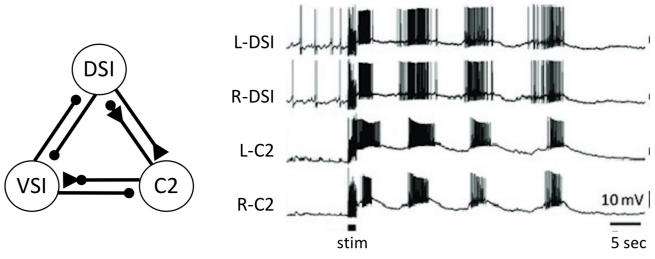

Fig. 1. A real frequency modulated CPG model. The neural circuit and swim motor patterns for the dorsal-ventral swimmer *Tritonia*. Left: The swim CPG consists of three neuron types: dorsal swim interneuron (DSI), cerebral neuron 2 (C2), and ventral swim interneuron (VSI). Right: Simultaneous intracellular microelectrode recordings show that two contralateral DSIs fire bursts of APs in phase with each other and slightly ahead of the two C2s. VSI (not recorded here) fires APs in the interburst interval. Courtesy of PNAS [2].

The author is with the School of Engineering, The University of Newcastle, Callaghan, NSW 2308, Australia. Tel: +61 2 4921 6352, Fax: +61 2 4921 6993 Email: zhiyong.chen@newcastle.edu.au.

The first motivation of this paper is to understand the synchronization phenomenon of frequency modulated signals observed in natural systems using mathematical language. Frequency modulation (FM) is one of most widely used technologies in engineering, and its potential advantages also motivate the research in this paper. For instance, conventional FM is the encoding of information in a carrier wave by varying the instantaneous frequency of the wave. It has a long history of applications in telecommunications, radio broadcasting, signal processing, and computing [3], [4], [5]. Compared with an amplitude modulation (AM) signal of equal power, FM has the advantage of providing a larger signal-to-noise ratio and, therefore, reducing radio frequency interference. Inspired by the biological CPGs discovered in animal locomotion, engineers have applied artificial CPGs as oscillator circuits in robotics [6], [7], [8]. These artificial CPGs can generate frequency modulated signals that resemble the firing bursts of APs to control robotic locomotion, the effectiveness of which has been well demonstrated even without a rigorous theoretical foundation. The exchange of frequency modulated signals is also an effective way to prevent transmission messages from disclosure. Examples of research on secure message transmission using neural circuits can be found in [9], [10].

However, there is a lack of mathematical principles, especially systems and control theories, for frequency modulated multi-agent systems. A multi-agent system (MAS) refers to a group of multiple dynamic entities (called agents) that share information or tasks to accomplish a common objective. The agents in an MAS can be circuits, autonomous vehicles, robots, power plants in an electrical grid, and other dynamic entities. A CPG network in its dynamic formulation is a typical MAS where each ganglion circuit (group of neurons) is regarded as an agent, and the agents generate patterned signals through inter-agent coordination. In real biological CPGs, the signals of burst firing are frequency modulated [11], [12], [13]. However, the mathematical principles of such CPGs have yet to be studied in terms of their coordinated behaviors. Research was mainly conducted based on simplified unmodulated CPG models. For example, the signals of burst firing are approximately represented by unmodulated sinusoidal-like waves when the adaptivity property of CPG circuits was studied for *Hirudo verbena*, a species of leech. Such an unmodulated leech CPG model was used in several references including [14], [15] to significantly reduce model complexity, as no systems or control theory exists for frequency modulated MASs.

Over the past two decades, many researchers have extensively studied MASs and achieved various outcomes. The research has been widely extended from the early work on simple dynamics to more general homogeneous MASs in the literature such as [16], [17], [18] for continuous-time systems and [19], [20], [21] for discrete-time systems. This line of research has also quickly spread to other related problems, such as synchronization, formation, flocking, swarming, and rendezvous [22], [23], [24]. It is well known that collective properties, in particular consensus, are closely related to the eigenvalues of the so-called Laplacian matrix, which in turn is crucially influenced by the network topology. It is fair to say that the existing control strategies for the analysis and control of linear homogeneous MASs are mature using basic Laplacian matrix properties in graph theory.

The mature solutions to various control problems for homogenous

MASs rely on the prerequisite that all the agents share common dynamics. Therefore, they mainly focus on trajectory synchronization. In the recent decade, researchers have put more efforts into the synchronization of complicated heterogeneous MASs, where the major challenge arises from the lack of common dynamics. To deal with this challenge, the work in [25], [26] assumes a common virtual exosystem that defines a trajectory to which all agents synchronize. Researchers have also studied the problem using different concepts of homogenization, such as in [27], [28]. Some other relevant techniques can be found in [29], [30].

Early research on nonlinear collective dynamic behaviors mainly addressed the synchronization of simply coupled nonlinear systems, such as the synchronization of master-slave chaotic systems [31], Kuramoto models [32], and coupled harmonic oscillators [33]. The solvability of the synchronization problem for general nonlinear heterogeneous MASs is the state of the art of this field. This problem was studied in [34], [35], [36] using a generalized output regulation framework under which the agents converge to specifically designed reference models. It was also formulated as a cooperative output regulation problem in a leader-following setting in the literature, such as [37], where the agents achieve synchronization on a trajectory that is assigned by one or more leaders. When the leader's system dynamics are unknown to some agents, adaptive schemes are developed, such as in [38], [39], [40]. These design approaches for heterogeneous MASs can be illustrated as reference consensus + agent-reference regulation, and they achieve the synchronized behaviors determined by the specified reference model dynamics (called virtual exosystem, exosystem, homogeneous model, internal model, reference model, or leader in difference references) rather than the inherent agent dynamics.

On the contrary, to adopt the inherent agent dynamics rather than the specified common dynamics, researchers have studied the dynamics consensus/synchronization problem, which is the prerequisite for trajectory synchronization. For example, the authors of [41], [42] proposed the concept of emergent dynamics, which is an average of the units' drifts. An MAS reaches dynamics consensus if the agents' trajectories converge to the one generated by the emergent dynamics. However, synchronization errors always exist in these works due to the heterogeneity between unit dynamics and emergent dynamics; this may be diminished by increasing the interconnection gain. The idea was also applied to Andronov-Hopf oscillators [43] and Stuart-Landau oscillators [44]. A more recent result on dynamics synchronization was developed in [45], [46] in a new formulation of autonomous synchronization. The result ensures that both the synchronized agent dynamics and the synchronized states are not specified a priori but autonomously determined by the inherent properties and the initial states of agents.

In all the references discussed in the above survey of MASs, the target of synchronization is formulated in terms of agent trajectories. This target can be achieved either directly through the exchange of trajectory information via network (homogeneous MASs) or indirectly through the consensus of specified or autonomous reference models plus regulation of agent trajectories to references (heterogeneous MASs). A key stumbling block in generalizing the existing MAS control techniques to frequency modulated MASs is that the techniques require direct or indirect exchange and coordination of unmodulated values of agent trajectories in the time domain. However, for frequency modulated MASs, the target is not determined by the instantaneous values of agent trajectories.

This paper is the first attempt to establish a framework for synchronization of frequency modulated MASs. The technical challenges lie in the fact that the frequency information is hidden from the instantaneous agent values that are observed or transmitted in a network. The analysis and control of frequency modulated MASs relies on an effective distributed frequency demodulation theory, which is still an open topic. Technically, we will first develop a new method to construct a frequency observer of a nonlinear system, especially subject to an external input representing synchronization error. None of the existing observer design methods is applicable in this scenario. Moreover, the gain from the external input to the observation error should be made arbitrarily small. Second, we will design a frequency synchronization approach, assuming the frequency observers work with appropriate observation errors. As the two actions occur concurrently, we will also ensure a deliberately formulated small-gain condition. The complete framework is established by an explicit controller architecture, supported by rigorous mathematical proof and demonstrated by numerical simulation.

The rest of the paper is organized as follows. The problem of synchronization of a frequency modulated MAS is formulated in Section II. A frequency observer for a nonlinear frequency modulated oscillator subject to network influence is designed in Section III. A frequency consensus algorithm is established via network interaction subject to observation errors in Section IV. Based on the techniques for frequency observation, frequency consensus, and examination of a small-gain condition, the overall solution to the synchronization problem is proposed in Section V. The effectiveness of the approach is verified in Section VI. Finally, the paper is concluded in Section VII.

II. Problem Formulation

This paper addresses a network of frequency modulated oscillators, also called agents, of the dynamics

$$\begin{aligned}\dot{\sigma}_i &= S\sigma_i + B\chi_i\\ \omega_i &= E\sigma_i + \omega_c\\ \dot{x}_i &= f(x_i)\omega_i + f_o(x_i),\ i = 1, \cdots, n,\end{aligned} \tag{1}$$

where $\sigma_i(t) \in \mathbb{R}^p$ is the state of the oscillator i. The information $E\sigma_i$ is modulated by a nonlinear carrier represented by the x_i-dynamics. In particular, $E\sigma_i$ is added to the carrier's base frequency ω_c to form the frequency $\omega_i(t) \in \mathbb{R}$ of the carrier. Then, the actual signal transmitted over the network becomes $x_i(t) \in \mathbb{R}^q$. The matrices S, B, and E are constant and of appropriate dimensions. The vector functions f and f_o are continuously differentiable and specified a priori. In particular, the function f satisfies $f(x_i) \neq 0$ for any $x_i \neq 0$ so that ω_i is effectively encoded in the signal x_i.

For example, Hindmarsh-Rose oscillators [47], which are a class of low-dimensional Hodgkin-Huxley model of neuronal activity, can characterize the spiking-bursting behavior of the membrane potential observed in experiments. The dynamics of a Hindmarsh-Rose oscillator are of the following form

$$\begin{bmatrix}\dot{v}_i\\ \dot{w}_i\\ \dot{z}_i\end{bmatrix} = \begin{bmatrix}c_1 v_i^2 - c_2 v_i^3 + w_i - z_i + c_I\omega_i\\ (-c_3 v_i^2 - w_i + c_4)\omega_i\\ c_5(c_6(v_i + c_7) - z_i)\end{bmatrix}, \tag{2}$$

where the variable $v_i(t) \in \mathbb{R}$ is the membrane potential, $w_i(t) \in \mathbb{R}$ is the spiking variable that measures the transport rate of sodium and potassium ions through fast ion channels, and $z_i(t) \in \mathbb{R}$ represents an adaptation current that is incremented at every spike, leading to a decrease in the firing rate. Model (2) has eight parameters: $c_1, \cdots, c_7$ and c_I, where the parameter c_I represents the current that enters the neuron. Using (2) as the carrier, the information ω_i is modulated as the frequency of the oscillator via the current c_I and the changing

This article has been accepted for publication in IEEE Transactions on Automatic Control. This is the author's version which has not been fully edited and content may change prior to final publication. Citation information: DOI 10.1109/TAC.2022.3197125

rate of the spiking variable w_i. It is noted that (2) is of the form (1) with

$$x_i = \begin{bmatrix} v_i \\ w_i \\ z_i \end{bmatrix},\ f(x_i) = \begin{bmatrix} c_I \\ -c_3 v_i^2 - w_i + c_4 \\ 0 \end{bmatrix},$$
$$f_o(x_i) = \begin{bmatrix} c_1 v_i^2 - c_2 v_i^3 + w_i - z_i \\ 0 \\ c_5(c_6(v_i + c_7) - z_i) \end{bmatrix}.$$

The objective is to design the input χ_i to each agent such that the states achieve synchronization in the sense of

$$\lim_{t\to\infty} \|\sigma_i(t) - \sigma_j(t)\| = 0,\ i, j = 1, \cdots, n, \tag{3}$$

or, in terms of the frequencies,

$$\lim_{t\to\infty} \|\omega_i(t) - \omega_j(t)\| = 0,\ i, j = 1, \cdots, n. \tag{4}$$

The design of χ_i relies on the signals received through a network. Associated with the network, we define a graph $\mathcal{G} = (\mathcal{V}, \mathcal{E}, A)$, where $\mathcal{V} = \{1, 2, \ldots, n\}$ indicates the vertex set, $\mathcal{E} \subseteq \mathcal{V} \times \mathcal{V}$ the edge set, and $A \in \mathbb{R}^{n\times n}$ the associated adjacency matrix whose (i, j) entry is a_{ij}. For $i, j \in \mathcal{V}$, $a_{ij} > 0$ if and only if $(i, j) \in \mathcal{E}$; otherwise, $a_{ij} = 0$. The set of neighbors of i is denoted as $\mathcal{N}_i = \{j \mid (i, j) \in \mathcal{E}\}$. Let the (i, j) entry of the Laplacian matrix $L \in \mathbb{R}^{n\times n}$ be l_{ij} where $l_{ii} = \sum_{j=1}^n a_{ij}$ and $l_{ij} = -a_{ij}$ for $i \neq j$, $i, j \in \mathcal{V}$.

If the oscillator states σ_i, $i \in \mathcal{V}$, were available for transmission, synchronization could be easily achieved by a controller of the form

$$\chi_i = -M \sum_{j\in\mathcal{N}_i} a_{ij}(\sigma_i - \sigma_j),\ i \in \mathcal{V} \tag{5}$$

with a certain network connectivity condition for a properly designed matrix M. However, in the present scenario, σ_j is not available for agent i. The controller under consideration is modified to

$$\chi_i = -M \sum_{j\in\mathcal{N}_i} a_{ij}(\sigma_i - \hat{\sigma}_j^i) \tag{6}$$
$$\hat{\sigma}_j^i = \mathcal{O}(x_j),\ j \in \mathcal{N}_i,\ i \in \mathcal{V}, \tag{7}$$

where $\hat{\sigma}_j^i$ is the estimated value of σ_j by agent i. The notation $\mathcal{O}(x_j)$ is not necessarily a static function but represents the output of a dynamic system whose input is x_j. The function of $\mathcal{O}(x_j)$ is to estimate the frequency ω_j and the oscillator state σ_j using the received signal x_j. In this sense, $\mathcal{O}(x_j)$ is called a frequency observer. The specific design of $\mathcal{O}(x_j)$ for each agent is motivated by the dynamics (1) and elaborated as follows:

$$\begin{aligned} \dot{\hat{\sigma}}_j^i &= S\hat{\sigma}_j^i + \mu(x_j, \hat{x}_j^i, \hat{\sigma}_j^i) \\ \hat{\omega}_j^i &= E\hat{\sigma}_j^i + \omega_c \\ \dot{\hat{x}}_j^i &= f(\hat{x}_j^i)\hat{\omega}_j^i + f_o(x_j) + \kappa(x_j, \hat{x}_j^i),\ j \in \mathcal{N}_i,\ i \in \mathcal{V} \end{aligned} \tag{8}$$

with $\hat{x}_j^i(0) = x_j(0)$ for some functions μ and κ. The aforementioned synchronization problem can be solved in a framework of three steps.

Step 1 (observer design): Let $\tilde{\sigma}_j^i = \hat{\sigma}_j^i - \sigma_j$, $j \in \mathcal{N}_i$, $i \in \mathcal{V}$, be the estimation errors. These errors can be put in a compact cumulative form of $\phi_i = \sum_{j\in\mathcal{N}_i} a_{ij}\tilde{\sigma}_j^i$ and $\phi = \mathrm{col}(\phi_1, \cdots, \phi_n)$. The operator $\mathrm{col}(\cdot)$ represents the column vector by stacking its arguments. Also, let $\sigma = \mathrm{col}(\sigma_1, \cdots, \sigma_n)$ and $\chi = \mathrm{col}(\chi_1, \cdots, \chi_n)$. As the system (1) is non-autonomous with an external input χ_i, the observer (8) is designed such that

$$\limsup_{t\to\infty} \|\phi(t)\| \leq \gamma_\sigma \limsup_{t\to\infty} \|\chi(t)\|$$

for some gain γ_σ.

Step 2 (perturbed consensus): The control input χ_i to each agent is designed such that consensus is achieved with the estimation error regarded as external perturbation in the sense of

$$\limsup_{t\to\infty} \|\chi(t)\| \leq \gamma_\chi \limsup_{t\to\infty} \|\phi(t)\|$$

for some gain γ_χ.

Step 3 (small-gain condition): The two gains γ_σ and γ_χ must satisfy a small-gain condition to ensure the final target of synchronization in terms of (3), which puts an extra constraint on the design in the above two steps.

The framework of these three steps will be developed in the subsequent three sections, respectively. The technical challenges in the development are summarized as follows.

(i) A new method is required to construct a frequency observer of a nonlinear system, which is especially subject to an external input. None of the existing observer design methods is applicable in this scenario. Moreover, the gain from the external input to the observation error can be made arbitrarily small.

(ii) To decouple the complexity of the overall system, we first consider Steps 1 and 2, separately. Step 1 can be achieved under the assumption that $\chi(t)$ is bounded, and similarly, Step 2 can be achieved under the assumption that $\phi(t)$ is bounded. Ensuring both assumptions occur concurrently in the closed-loop system through a certain interconnection is considered a technical difficulty. If these bounded assumptions are satisfied, the proposed controller must also ensure a small-gain condition, which requires a deep understanding of the coupling structure in the system dynamics. It is worth mentioning that both synchronization and consensus address the agreement among agents, and there is no strict boundary between the two terms. The overall problem in this paper is called synchronization, as it is studied for the full complicated dynamics (1), whereas the sub-problem in Step 2 is called consensus, as only the simpler σ_i-dynamics are considered in this step. This terminology follows the meaningful categorization given in [16].

(iii) Among the agents, the communicated state is the modulated signal x_i; however, the target of the control strategy is the synchronization of the state σ_i. In fact, the synchronization of the instantaneous values of x_i is not needed in this framework. Therefore, the existing synchronization methods for nonlinear systems using a reference model (or an internal model) do not apply in the present setting.

III. Design of a Frequency Observer

In this section, we study a frequency observer for a frequency modulated oscillator. To simplify the notation, we omit the subscripts and superscripts in this section by focusing on an individual scenario. More specially, we consider the model

$$\begin{aligned} \dot{\sigma} &= S\sigma + B\chi \\ \omega &= E\sigma + \omega_c \\ \dot{x} &= f(x)\omega + f_o(x) \end{aligned} \tag{9}$$

and the corresponding observer

$$\begin{aligned} \dot{\hat{\sigma}} &= S\hat{\sigma} + \mu(x, \hat{x}, \hat{\sigma}) \\ \hat{\omega} &= E\hat{\sigma} + \omega_c \\ \dot{\hat{x}} &= f(\hat{x})\hat{\omega} + f_o(x) + \kappa(x, \hat{x}) \end{aligned} \tag{10}$$

with $\hat{x}(0) = x(0)$. The following notations are used throughout the paper. For a real symmetric matrix P, let $\lambda_{\max}(P)$ and $\lambda_{\min}(P)$ be the maximum and minimum eigenvalues of P, respectively. And let $\varpi(P) = \frac{\lambda_{\max}(P)}{\lambda_{\min}(P)}$.

Lemma 3.1: Consider the dynamics (9) *and the observer* (10) *with a constant* $\omega_c > 0$ *and a time varying signal* $\chi(t)$ *satisfying* $\|\chi(t)\| \le b_\chi,\ \forall t \ge 0$ *for a constant* b_χ*. Suppose the frequency modulated signal* $x(t)$ *is bounded, i.e.,* $\underline{\alpha} \le \|x(t)\| \le \bar{\alpha}, \forall t \ge 0$*, for some constants* $\underline{\alpha}, \bar{\alpha} > 0$*. Given any constants* $b_o, \gamma > 0$*, if there exist matrices* K_o *and* $P = P^\mathsf{T} > 0$ *such that*

$$\begin{aligned} P(S - K_o E) + (S - K_o E)^\mathsf{T} P &= -I \\ \|PB\|\sqrt{\varpi(P)} &< \gamma_o \end{aligned} \tag{11}$$

for $\gamma_o = \gamma/8$*, then there exist control functions* μ *and* κ *such that*

$$\limsup_{t\to\infty} \|\hat{\sigma}(t) - \sigma(t)\| \le \gamma \limsup_{t\to\infty} \|\chi(t)\| \tag{12}$$

for

$$\hat{x}(0) = x(0),\ \|\hat{\sigma}(0) - \sigma(0)\| \le b_o. \tag{13}$$

Proof: The proof is constructive by explicitly providing the functions μ and κ that define the frequency observer. For the convenience of presentation, denote the observation errors $\tilde{\sigma} = \hat{\sigma} - \sigma$ and $\tilde{x} = \hat{x} - x$. With the relationship $\hat{\omega} - \omega = E\tilde{\sigma}$, the error dynamics can be written as

$$\begin{aligned} \dot{\tilde{\sigma}} &= S\tilde{\sigma} + \mu(x, \hat{x}, \hat{\sigma}) - B\chi \\ \dot{\tilde{x}} &= f(\hat{x})\hat{\omega} - f(x)\omega + \kappa(x, \hat{x}) \\ &= f(x)E\tilde{\sigma} + [f(\hat{x}) - f(x)]\hat{\omega} + \kappa(x, \hat{x}). \end{aligned}$$

As S is not necessarily Hurwitz, it is difficult to directly analyze the stability of the above $(\tilde{\sigma}, \tilde{x})$-system. Therefore, we introduce a new variable

$$\nu = \tilde{\sigma} - K(\hat{x})\tilde{x}, \tag{14}$$

for a matrix function $K(\hat{x})$, that results in the $(\nu, \tilde{x})$-system in the new coordinate.

The remaining proof is divided into three steps. In Step 1, we will give the explicit constructions of K, μ, and κ such that the $(\nu, \tilde{x})$-system has a certain structure to facilitate the stability analysis in the subsequent steps. The property $\|\tilde{x}(t)\| < b_x,\ \forall t \ge 0$, for a certain constant b_x is a prerequisite for stability analysis and will be proved in Step 2. Meanwhile, two Lyapunov-like functions for the two subsystems governing ν and $\tilde{x}$ will be constructed, respectively. In Step 3, the two Lyapunov-like functions will be combined to form an overall Lyapunov function for the complete $(\nu, \tilde{x})$-system and hence complete the proof.

Step 1: Pick a matrix function

$$K(\hat{x}) = K_o \frac{f^\mathsf{T}(\hat{x})}{\|f(\hat{x})\|^2}. \tag{15}$$

It will be proved later that $\|f(\hat{x}(t))\| > 0,\ \forall t \ge 0$, to validate the definition of K. Direct calculation shows that

$$K(\hat{x})f(\hat{x}) = K_o \frac{f^\mathsf{T}(\hat{x})}{\|f(\hat{x})\|^2} f(\hat{x}) = K_o.$$

Then, one has

$$S\tilde{\sigma} - K(\hat{x})f(\hat{x})E\tilde{\sigma} = S\tilde{\sigma} - K_o E\tilde{\sigma} = \bar{S}\tilde{\sigma},$$

where $\bar{S} = S - K_o E$ is Hurwitz with (11) that can be rewritten as

$$\begin{aligned} P\bar{S} + \bar{S}^\mathsf{T} P &= -I \\ 8\|PB\|\sqrt{\varpi(P)} &< \gamma. \end{aligned} \tag{16}$$

The new variable ν defined in (14) gives

$$\begin{aligned} \dot{\nu} =& S\tilde{\sigma} + \mu(x, \hat{x}, \hat{\sigma}) - B\chi \\ & - K(\hat{x})[f(x)E\tilde{\sigma} + [f(\hat{x}) - f(x)]\hat{\omega} + \kappa(x, \hat{x})] \\ & - \dot{K}(\hat{x})\tilde{x} \\ =& S\tilde{\sigma} - K(\hat{x})f(x)E\tilde{\sigma} + \bar{\mu}(x, \hat{x}) - B\chi \\ =& S\tilde{\sigma} - K(\hat{x})f(\hat{x})E\tilde{\sigma} - K(\hat{x})f(x)E\tilde{\sigma} \\ & + K(\hat{x})f(\hat{x})E\tilde{\sigma} + \bar{\mu}(x, \hat{x}) - B\chi \\ =& \bar{S}\tilde{\sigma} + K(\hat{x})[f(\hat{x}) - f(x)]E\tilde{\sigma} + \bar{\mu}(x, \hat{x}) - B\chi, \end{aligned}$$

where

$$\begin{aligned} \mu(x, \hat{x}, \hat{\sigma}) =& K(\hat{x})\kappa(x, \hat{x}) + K(\hat{x})[f(\hat{x}) - f(x)]\hat{\omega} \\ & + K'(x, \hat{x}, \hat{\sigma})(\hat{x} - x) + \bar{\mu}(x, \hat{x}) \\ \bar{\mu}(x, \hat{x}) =& -\bar{S}K(\hat{x})(\hat{x} - x) \\ & - K(\hat{x})[f(\hat{x}) - f(x)]EK(\hat{x})(\hat{x} - x) \end{aligned}$$

and

$$\begin{aligned} K'(x, \hat{x}, \hat{\sigma}) =& K_o \Bigg(\frac{\|f(\hat{x})\|^2 I_q - 2f(\hat{x})f^\mathsf{T}(\hat{x})}{\|f(\hat{x})\|^4} \times \\ & \frac{\partial f(\hat{x})}{\partial \hat{x}} \left(f(\hat{x})(E\hat{\sigma} + \omega_c) + f_o(x) + \kappa(x, \hat{x})\right) \Bigg)^\mathsf{T}. \end{aligned}$$

It is noted that, along the trajectory of (10), one has

$$\dot{K}(\hat{x}) = \frac{\partial K(\hat{x})}{\partial \hat{x}} \dot{\hat{x}} = K'(x, \hat{x}, \hat{\sigma}).$$

The ν-dynamics can be further simplified to

$$\dot{\nu} = \bar{S}\nu + K(\hat{x})[f(\hat{x}) - f(x)]E\nu - B\chi. \tag{17}$$

Next, by $E\tilde{\sigma} = E\nu + EK(\hat{x})\tilde{x}$, the $\tilde{x}$-dynamics can be rewritten as

$$\dot{\tilde{x}} = f(x)E\nu - \beta\tilde{x} \tag{18}$$

using the function

$$\kappa(x, \hat{x}) = -\beta\tilde{x} - f(x)EK(\hat{x})\tilde{x} - [f(\hat{x}) - f(x)]\hat{\omega},$$

where β is to be specified later.

As f is continuously differentiable, there exist positive numbers $\alpha, \theta > 0$ such that (see Lemma 11.1 of [48])

$$\begin{aligned} \|[f(x + \tilde{x}) - f(x)]E\nu\| &\le \theta\|\nu\|\|\tilde{x}\| \\ \|f(x)E\nu\| &\le \theta\alpha\|\nu\|,\ \forall \underline{\alpha} \le \|x\| \le \bar{\alpha},\ \|\tilde{x}\| \le \underline{\alpha}/2. \end{aligned}$$

We define two positive numbers $b_x, b_K > 0$ as

$$\begin{aligned} b_x = \arg \max_{b \le \underline{\alpha}/2} \{ & 8\theta\|PK(x + \tilde{x})\|\|\tilde{x}\| \le 1,\ \forall \underline{\alpha} \le \|x\| \le \bar{\alpha}, \\ & \|\tilde{x}\| \le b\} \end{aligned} \tag{19}$$

and

$$b_K = \max_{\underline{\alpha} \le \|x\| \le \bar{\alpha}, \|\tilde{x}\| \le b_x} \|K(x + \tilde{x})\|. \tag{20}$$

We also define a function

$$c(\tilde{x}) = \max_{\underline{\alpha} \le \|x\| \le \bar{\alpha}} \{8\theta\|PK(x + \tilde{x})\|\|\tilde{x}\|\}.$$

Since $c(0) = 0$, one has $c(\tilde{x}) \le 1, \forall \|\tilde{x}\| \le b$, for a sufficiently small parameter $b > 0$. The number b_x is defined as the largest value of the parameter b in the interval $(0, \underline{\alpha}/2]$. From this definition, one has $b_x \le \underline{\alpha}/2$. For $\underline{\alpha} \le \|x\| \le \bar{\alpha}$ and $\|\tilde{x}\| \le b_x$, one has

$\underline{\alpha}/2 \le \|\tilde{x}+x\| \le \bar{\alpha}+\underline{\alpha}/2$. As a result, b_K is finite according to the definition of the function K. Let β satisfy the following conditions

$$\beta > \frac{\varpi(P)b_o^2 + 8\|PB\|^2 b_\chi^2 \varpi(P)}{4b_x^2} + \theta^2\alpha^2 \tag{21}$$

$$\beta > \frac{b_K^2}{4} + \theta^2\alpha^2 \tag{22}$$

$$\beta \ge \frac{1}{8\lambda_{\min}(P)} + 2\lambda_{\min}(P)\theta^2\alpha^2. \tag{23}$$

The remaining analysis will be conducted on the interconnected system composed of (17) and (18).

Step 2: We will prove

$$\|\tilde{x}(t)\| < b_x,\ \forall t \ge 0. \tag{24}$$

If (24) does not hold, there exists a finite time $T > 0$ such that $\|\tilde{x}(t)\| < b_x,\ \forall t \in [0, T)$, and $\|\tilde{x}(T)\| = b_x$, because $\|\tilde{x}(0)\| = 0$ and $\tilde{x}(t)$ is a continuous function of t. A contradiction will be derived below.

First, for the system (17), pick a Lyapunov function candidate $V_1(\nu) = \nu^\mathsf{T} P\nu$, whose time derivative satisfies

$$\begin{aligned}\dot{V}_1(\nu) =& -\|\nu\|^2 + 2\nu^\mathsf{T} PK(x+\tilde{x})[f(\hat{x}) - f(x)]E\nu - 2\nu^\mathsf{T} PB\chi \\ \le& -\|\nu\|^2 + 2\theta\|PK(x+\tilde{x})\|\|\tilde{x}\|\|\nu\|^2 \\ &+ \frac{1}{4}\|\nu\|^2 + 4\|PB\|^2\|\chi\|^2.\end{aligned}$$

For $t \in [0, T]$, one has $\|\tilde{x}(t)\| \le b_x$ and hence $8\theta\|PK(x+\tilde{x})\|\|\tilde{x}\| \le 1$. Therefore,

$$\begin{aligned}\dot{V}_1(\nu) \le& -\|\nu\|^2 + \frac{1}{4}\|\nu\|^2 + \frac{1}{4}\|\nu\|^2 + 4\|PB\|^2\|\chi\|^2 \\ \le& -\frac{1}{2}\|\nu\|^2 + 4\|PB\|^2\|\chi\|^2\end{aligned} \tag{25}$$

and

$$\dot{V}_1(\nu) \le -\frac{1}{2\lambda_{\max}(P)}V_1(\nu) + 4\|PB\|^2\|\chi\|^2. \tag{26}$$

From (26), the comparison principle gives

$$\begin{aligned}&V_1(\nu(t)) \\ \le& V_1(\nu(0)) + 4\|PB\|^2\int_0^t \exp(-\frac{1}{2\lambda_{\max}(P)}(t-\tau))\|\chi(\tau)\|^2 d\tau \\ \le& V_1(\nu(0)) + 4\|PB\|^2 b_\chi^2\int_0^t \exp(-\frac{1}{2\lambda_{\max}(P)}(t-\tau))d\tau \\ =& V_1(\nu(0)) + 8\|PB\|^2 b_\chi^2\lambda_{\max}(P)\left[1 - \exp(-\frac{1}{2\lambda_{\max}(P)}t)\right] \\ \le& V_1(\nu(0)) + 8\|PB\|^2 b_\chi^2\lambda_{\max}(P) \\ \le& \lambda_{\max}(P)\|\nu(0)\|^2 + 8\|PB\|^2 b_\chi^2\lambda_{\max}(P).\end{aligned}$$

From the above calculation, one has

$$\begin{aligned}\lambda_{\min}(P)\|\nu(t)\|^2 \le& V_1(\nu(t)) \\ \le& \lambda_{\max}(P)\|\nu(0)\|^2 + 8\|PB\|^2 b_\chi^2\lambda_{\max}(P),\end{aligned}$$

and then

$$\|\nu(t)\|^2 \le \varpi(P)\|\nu(0)\|^2 + 8\|PB\|^2 b_\chi^2\varpi(P). \tag{27}$$

By (13) and the fact

$$\nu(0) = \tilde{\sigma}(0) - K(\hat{x}(0))\tilde{x}(0) = \tilde{\sigma}(0),$$

(27) implies

$$\|\nu(t)\|^2 \le \varpi(P)b_o^2 + 8\|PB\|^2 b_\chi^2\varpi(P). \tag{28}$$

Secondly, for the system (18), pick a Lyapunov function candidate $V_2(\tilde{x}) = \|\tilde{x}\|^2/2$, whose time derivative satisfies

$$\begin{aligned}\dot{V}_2(\tilde{x}) =& -\beta\|\tilde{x}\|^2 + \tilde{x}^\mathsf{T} f(x)E\nu \\ \le& -\beta\|\tilde{x}\|^2 + \theta\alpha\|\tilde{x}\|\|\nu\| \\ \le& -(\beta - \theta^2\alpha^2)\|\tilde{x}\|^2 + \frac{1}{4}\|\nu\|^2 \\ \le& -2(\beta - \theta^2\alpha^2)V_2(\tilde{x}) + \frac{1}{4}\|\nu\|^2.\end{aligned} \tag{29}$$

It is noted that $\beta - \theta^2\alpha^2 > 0$ from (21) or (22). Applying the comparison principle again gives

$$\begin{aligned}&V_2(\tilde{x}(t)) \\ \le& V_2(\tilde{x}(0)) + \frac{1}{4}\int_0^t \exp(-2(\beta - \theta^2\alpha^2)(t-\tau))\|\nu(\tau)\|^2 d\tau \\ \le& \frac{\varpi(P)b_o^2 + 8\|PB\|^2 b_\chi^2\varpi(P)}{4}\int_0^t \exp(-2(\beta - \theta^2\alpha^2)(t-\tau))d\tau \\ \le& \frac{\varpi(P)b_o^2 + 8\|PB\|^2 b_\chi^2\varpi(P)}{8(\beta - \theta^2\alpha^2)}[1 - \exp(-2(\beta - \theta^2\alpha^2)t)] \\ \le& \frac{\varpi(P)b_o^2 + 8\|PB\|^2 b_\chi^2\varpi(P)}{8(\beta - \theta^2\alpha^2)},\end{aligned}$$

where (28) is used in the above calculation. By (21), one has

$$\|\tilde{x}(t)\|^2 = 2V_2(\tilde{x}(t)) \le \frac{\varpi(P)b_o^2 + 8\|PB\|^2 b_\chi^2\varpi(P)}{4(\beta - \theta^2\alpha^2)} < b_x^2$$

for $t \in [0, T]$. It is a contradiction with $\|\tilde{x}(T)\| = b_x$. From the above argument, one has (24) proved. Also, $\|K(\hat{x}(t))\| \le b_K$, $\hat{x}(t) \ne 0$, $f(\hat{x}(t)) \ne 0$, (25), and (29) hold for all $t \ge 0$. The definition of K in (15) is thus validated.

Step 3: As (22) is equivalent to

$$\sqrt{\frac{1}{4(\beta - \theta^2\alpha^2)}} < \frac{1}{b_K},$$

(29) implies that the $\tilde{x}$-system (18) is input-to-state stable viewing $\tilde{x}$ as the state and ν as the input, and particularly (see Theorem 2.7 of [48]),

$$\limsup_{t\to\infty}\|\tilde{x}(t)\| \le \frac{1}{b_K}\limsup_{t\to\infty}\|\nu(t)\|.$$

Hence, the following inequalities hold

$$\limsup_{t\to\infty}\|K(\hat{x}(t))\tilde{x}(t)\| \le b_K\limsup_{t\to\infty}\|\tilde{x}(t)\| \le \limsup_{t\to\infty}\|\nu(t)\|. \tag{30}$$

For $\bar{V}_2(\tilde{x}) = \lambda_{\min}(P)\|\tilde{x}\|^2$, a variant of (29) is written as follows

$$\begin{aligned}\dot{\bar{V}}_2(\tilde{x}) =& -2\lambda_{\min}(P)\beta\|\tilde{x}\|^2 + 2\lambda_{\min}(P)\tilde{x}^\mathsf{T} f(x)E\nu \\ \le& -2\lambda_{\min}(P)\beta\|\tilde{x}\|^2 + 2\lambda_{\min}(P)\theta\alpha\|\tilde{x}\|\|\nu\| \\ \le& -(2\lambda_{\min}(P)\beta - 4\lambda_{\min}^2(P)\theta^2\alpha^2)\|\tilde{x}\|^2 + \frac{1}{4}\|\nu\|^2.\end{aligned} \tag{31}$$

It is ready to construct the composite Lyapunov function

$$V(\nu, \tilde{x}) = V_1(\nu) + \bar{V}_2(\tilde{x})$$

that satisfies

$$\begin{aligned}\lambda_{\min}(P)\|\operatorname{col}(\nu, \tilde{x})\|^2 \le& V(\nu, \tilde{x}) \\ \le& \lambda_{\max}(P)\|\nu\|^2 + \lambda_{\min}(P)\|\tilde{x}\|^2 \\ \le& \lambda_{\max}(P)\|\operatorname{col}(\nu, \tilde{x})\|^2.\end{aligned}$$

Using (25) and (31), the derivative of $V(\nu,\tilde{x})$ satisfies

$$\begin{aligned}\dot{V}(\nu,\tilde{x}) \leq & -\frac{1}{4}\|\nu\|^2-(2\lambda_{\min}(P)\beta-4\lambda_{\min}^2(P)\theta^2\alpha^2)\|\tilde{x}\|^2\\ &+4\|PB\|^2\|\chi\|^2\\ \leq & -\frac{1}{4}\|\operatorname{col}(\nu,\tilde{x})\|^2+4\|PB\|^2\|\chi\|^2\end{aligned}$$

noting $\lambda_{\min}(P)\beta-2\lambda_{\min}^2(P)\theta^2\alpha^2\geq 1/8$ according to (23). As a result, the $(\nu,\tilde{x})$-system composed of (17) and (18) is input-to-state stable viewing $(\nu,\tilde{x})$ as the state and χ as the input. In particular, one has

$$\limsup_{t\to\infty}\|\operatorname{col}(\nu(t),\tilde{x}(t))\|\leq\gamma/2\limsup_{t\to\infty}\|\chi(t)\| \tag{32}$$

as (16) is equivalent to

$$\frac{\gamma}{2}>\sqrt{\frac{\lambda_{\max}(P)4\|PB\|^2}{\lambda_{\min}(P)/4}}=4\|PB\|\sqrt{\varpi(P)}.$$

Finally, using (14), (30), and (32), the following conclusion is verified

$$\begin{aligned}&\limsup_{t\to\infty}\|\tilde{\sigma}(t)\|\\ \leq&\limsup_{t\to\infty}\|\nu(t)\|+\limsup_{t\to\infty}\|K(\hat{x}(t))\tilde{x}(t)\|\\ \leq&2\limsup_{t\to\infty}\|\nu(t)\|\leq 2\limsup_{t\to\infty}\|\operatorname{col}(\nu(t),\tilde{x}(t))\|\\ \leq&\gamma\limsup_{t\to\infty}\|\chi(t)\|,\end{aligned}$$

which is (12). The proof is thus completed. □

Remark 3.1: The design of a state observer is an important topic in control theory. There are many practical applications of Luenberger observers and Kalman filters. Researchers have also studied many nonlinear observer design methods. For example, the observer in [49] is based on an observer error linearization approach developed in the paper. An extended Luenberger observer was designed in [50] using the technique of linearization and transformation into a nonlinear observer canonical form. However, these linearization-based methods are valid only in a neighborhood of an initial state. High-gain observers were studied in many references, such as [51], [52], for nonlinear systems of canonical observability form. They do not apply in the present paper, as the systems under consideration do not have a canonical form. The new approach takes advantage of the interconnection structure between the σ and x subsystems and derives a Lyapunov function-based argument. Moreover, the observer designed in this paper allows an arbitrarily specified gain γ from the external input to the estimation error as in (12), which has not been studied using any of the existing observer design approaches.

Remark 3.2: The gain from $\|\chi\|$ to the estimation error $\|\hat{\sigma}-\sigma\|$ is characterized in Lemma 3.1 by an appropriately designed observer. It is noted that the influence of χ can be completely removed by compensation in the observer (10) such as $\dot{\hat{\sigma}}=S\hat{\sigma}+B\chi+\mu(x,\hat{x},\hat{\sigma})$. However, such compensation is not applicable when the observer is used for network synchronization in this paper. Consider the observer (8) of agent i to estimate the frequency of agent j. The only signal agent i is able to access is the state x_j, not the input χ_j of agent j.

Remark 3.3: It is assumed that the frequency modulated signal $x(t)$ is bounded, i.e., $\underline{\alpha}\leq\|x(t)\|\leq\bar{\alpha},\forall t\geq 0$, in Lemma 3.1. It is a reasonable assumption for a persistently exciting oscillator. For example, for an oscillator

$$\dot{x}=\begin{bmatrix}0&\omega(t)\\-\omega(t)&0\end{bmatrix}x,$$

one has $\|x(t)\|=\|x(0)\|,\ \forall t\geq 0$, according to

$$\frac{d\|x(t)\|^2}{dt}=2x^{\mathsf{T}}\dot{x}=2x^{\mathsf{T}}\begin{bmatrix}0&\omega(t)\\-\omega(t)&0\end{bmatrix}x=0.$$

It means that $x(t)$ is bounded, no matter how $\omega(t)$ varies. Oscillation is also typically generated as a stable limit cycle, which is a closed trajectory and bounded. For example, a Hindmarsh-Rose oscillator of the dynamics

$$\begin{bmatrix}\dot{v}\\\dot{w}\\\dot{z}\end{bmatrix}=\begin{bmatrix}v^2-v^3+w-z+\omega(t)\\(-v^2-w+1)\omega(t)\\v+1-z\end{bmatrix}$$

has a bounded trajectory $x(t)=[v(t),w(t),z(t)]^{\mathsf{T}}$ for any $\omega(t):\mathbb{R}\mapsto[\underline{\omega},\bar{\omega}]$ with $\underline{\omega},\bar{\omega}>0$. Indeed, for $\hat{x}(t)=[v(t),\hat{w}(t),z(t)]^{\mathsf{T}}$ with $\hat{w}(t)=(\sqrt{\underline{\omega}}/\bar{\omega})w(t)$, one has

$$\begin{aligned}\frac{d\|\hat{x}(t)\|^2}{dt}\leq&2v^3-2v^4+4v^2/(\underline{\omega}/\bar{\omega})^2+(\underline{\omega}/\bar{\omega})^2w^2/4+2v^2\\ &+z^2/2+\bar{\omega}^2+v^2+v^4-(\underline{\omega}/\bar{\omega})^2w^2/2+2\\ &+2v^2+2-z^2\\ \leq&-\frac{\min\{\underline{\omega},1\}}{4}\|\hat{x}\|^2+c\end{aligned}$$

for a constant $c=(4(\bar{\omega}/\underline{\omega})^2+7)^2+\bar{\omega}^2+4+1/16$. It implies that $\|\hat{x}(t)\|$ is bounded, so is $\|x(t)\|$. The explicit calculation of the bounds of $\|x(t)\|$, i.e., $\underline{\alpha}$ and $\bar{\alpha}$, are usually difficult and conservative. Therefore, numerical measurement of the bounds is more practically feasible for complicated oscillators.

To close this section, we discuss the existence of the solution to (11) for a special case where the information to be modulated is a general sinusoidal signal $\omega(t)=a\sin(\varsigma t+\theta)$. It is obvious that such a signal can be generated by the model

$$\dot{\sigma}=\begin{bmatrix}0&\varsigma\\-\varsigma&0\end{bmatrix}\sigma,\ \omega=\begin{bmatrix}1&0\end{bmatrix}\sigma,\ \sigma(0)=\begin{bmatrix}a\sin(\theta)\\a\cos(\theta)\end{bmatrix}.$$

The specific matrices S and E used for this model are given in the following corollary.

Corollary 3.1: For

$$S=\begin{bmatrix}0&\varsigma\\-\varsigma&0\end{bmatrix},\ E=\begin{bmatrix}1&0\end{bmatrix},\ B=\begin{bmatrix}b_1\\b_2\end{bmatrix},$$

with $\varsigma,b_1,b_2>0$ and any constant $\gamma_o>0$, there exist matrices K_o and $P=P^{\mathsf{T}}>0$ such that (11) *is satisfied.* ∎

Proof: For a positive ρ and $b=b_1/b_2$, let

$$K_o=\begin{bmatrix}\frac{b^2+1}{2}b\rho+b\varsigma\\\frac{b^2+1}{2}\rho-\varsigma\end{bmatrix}.$$

Then,

$$\bar{S}=S-K_oE=\begin{bmatrix}-\frac{b^2+1}{2}b\rho-b\varsigma&\varsigma\\-\frac{b^2+1}{2}\rho&0\end{bmatrix}.$$

We can solve the equation in (11) as

$$P=\frac{1}{2\varsigma b}\begin{bmatrix}1&-b\\-b&\frac{b^2\rho+2\varsigma}{\rho}\end{bmatrix}.$$

The characteristic equation of P is

$$\det(P-\lambda I)=\lambda^2-\frac{(b^2+1)\rho+2\varsigma}{2b\rho\varsigma}\lambda+\frac{1}{2b^2\rho\varsigma}=0,$$

which implies that P has two positive real eigenvalues and hence is positive definite. Moreover,

$$\begin{aligned}\varpi(P) <&\varpi(P)+\varpi^{-1}(P)=\frac{\lambda_{\max}(P)}{\lambda_{\min}(P)}+\frac{\lambda_{\min}(P)}{\lambda_{\max}(P)}\\ =&\frac{(b^2+1)^2\rho/2+2\varsigma^2/\rho+2b^2\varsigma}{\varsigma}.\end{aligned}$$

It is noted that $\|PB\|=b_2/(\rho b)$. Then,

$$\begin{aligned}\|PB\|^2\varpi(P)<&\frac{(b^2+1)^2/2+2\varsigma^2/\rho^2+2b^2\varsigma/\rho}{\rho\varsigma b^2/b_2^2}\\ \le&\frac{(b^2+1)^2/2+2\varsigma^2+2b^2\varsigma}{\rho\varsigma b^2/b_2^2}\le\gamma_o^2\end{aligned}$$

for

$$\rho\ge\max\{1,\frac{(b^2+1)^2/2+2\varsigma^2+2b^2\varsigma}{\gamma_o^2\varsigma b^2/b_2^2}\}.$$

The proof is thus completed. □

IV. Perturbed Consensus

Consider the σ_i-dynamics of the system (1), that is,

$$\dot\sigma_i=S\sigma_i+B\chi_i,\ i\in\mathcal{V}. \tag{33}$$

If the states σ_i, $i\in\mathcal{V}$, were directly transferred over the network, without frequency modulation, the synchronization target (3) could be easily achieved by the ideal controller (5). However, with frequency modulation, the controller takes the form (6), where the estimated state $\hat\sigma_j^i$ rather than σ_j is available for the design. The controller (6) can be rewritten as the ideal controller (5) subject to perturbation (i.e., the estimation error),

$$\chi_i=-M\sum_{j\in\mathcal{N}_i}a_{ij}(\sigma_i-\sigma_j)+M\sum_{j\in\mathcal{N}_i}a_{ij}\tilde\sigma_j^i,\ i\in\mathcal{V}. \tag{34}$$

For $\phi_i=\sum_{j\in\mathcal{N}_i}a_{ij}\tilde\sigma_j^i$, the system composed of (33) and (34) becomes

$$\dot\sigma_i=S\sigma_i-BM\sum_{j\in\mathcal{N}_i}a_{ij}(\sigma_i-\sigma_j)+BM\phi_i,\ i\in\mathcal{V}. \tag{35}$$

Let $\mathbf{r},\mathbf{1}\in\mathbb{R}^n$ be the left and right eigenvectors corresponding to the eigenvalue zero of the Laplacian matrix L and satisfying $\mathbf{r}^{\mathsf{T}}\mathbf{1}=1$. There exist matrices $W\in\mathbb{R}^{(n-1)\times n}$ and $U\in\mathbb{R}^{n\times(n-1)}$ such that

$$T=\left[\begin{array}{c}\mathbf{r}^{\mathsf{T}}\\ W\end{array}\right],\ T^{-1}=\left[\begin{array}{cc}\mathbf{1}&U\end{array}\right], \tag{36}$$

$W\mathbf{1}=0$ and $\mathbf{r}^{\mathsf{T}}U=0$. As a result,

$$TLT^{-1}=\left[\begin{array}{cc}0&0\\0&H\end{array}\right], \tag{37}$$

where

$$H=WLU \tag{38}$$

is called an H-matrix associated with L. It is well known that, under Assumption 1 given below, all the eigenvalues of H have positive real parts.

Assumption 1: The directed graph $\mathcal{G}$ contains a spanning tree. ∎

To ensure the solvability of the consensus problem, the following assumption is also needed.

Assumption 2: The pair of matrices (S,B) is stabilizable. ∎

Now, the main result about perturbed consensus is given in the following lemma.

Lemma 4.1: Consider the system (33) *with* (34) *under Assumptions 1 and 2. If M is selected such that*

$$A_\varsigma=I_{n-1}\otimes S-H\otimes BM \tag{39}$$

is Hurwitz, then there exists a constant γ_χ such that

$$\limsup_{t\to\infty}\|\chi(t)\|\le\gamma_\chi\limsup_{t\to\infty}\|\phi(t)\| \tag{40}$$

for any bounded $\phi(t)$. In particular, let $Q=Q^{\mathsf{T}}>0$ be the solution to the Lyapunov equation

$$QA_\varsigma+A_\varsigma^{\mathsf{T}}Q=-2I. \tag{41}$$

Then, $\gamma_\chi=\|M\|(\sqrt{\varpi(Q)}\|LU\|\|Q(W\otimes BM)\|+1)$.

Proof: The system composed of (33) and (34), i.e., (35), can be put in a compact form

$$\dot\sigma=(I_n\otimes S-L\otimes BM)\sigma+(I_n\otimes BM)\phi. \tag{42}$$

We introduce the following coordinate transformation

$$\left[\begin{array}{c}\bar\sigma\\ \zeta\end{array}\right]=(T\otimes I_p)\,\sigma,\ \sigma=\left(T^{-1}\otimes I_p\right)\left[\begin{array}{c}\bar\sigma\\ \zeta\end{array}\right]. \tag{43}$$

In the new coordinate, the system (42) is equivalent to

$$\left[\begin{array}{c}\dot{\bar\sigma}\\ \dot\zeta\end{array}\right]=(I_n\otimes S-TLT^{-1}\otimes BM)\left[\begin{array}{c}\bar\sigma\\ \zeta\end{array}\right]+(T\otimes BM)\phi,$$

that is

$$\begin{aligned}\dot{\bar\sigma}&=S\bar\sigma+(\mathbf{r}^{\mathsf{T}}\otimes BM)\phi\\ \dot\zeta&=A_\varsigma\zeta+(W\otimes BM)\phi.\end{aligned} \tag{44}$$

The derivative of the function

$$V(\zeta)=\zeta^{\mathsf{T}}Q\zeta, \tag{45}$$

along the trajectories of (44), is

$$\begin{aligned}\dot V(\zeta)=&-2\|\zeta\|^2+2\zeta^{\mathsf{T}}Q(W\otimes BM)\phi\\ =&-\|\zeta\|^2+\|Q(W\otimes BM)\|^2\|\phi\|^2.\end{aligned} \tag{46}$$

It implies that the ζ-system (44) is input-to-state stable viewing ζ as the state and ϕ as the input. In particular,

$$\limsup_{t\to\infty}\|\zeta(t)\|\le\gamma_\zeta\limsup_{t\to\infty}\|\phi(t)\| \tag{47}$$

for

$$\gamma_\zeta=\sqrt{\varpi(Q)}\|Q(W\otimes BM)\|. \tag{48}$$

Next, from the relationship

$$(L\otimes M)\sigma=(LT^{-1}\otimes M)\left[\begin{array}{c}\bar\sigma\\ \zeta\end{array}\right]=(LU\otimes M)\zeta,$$

one has

$$\begin{aligned}\limsup_{t\to\infty}\|(L\otimes M)\sigma(t)\|\le&\|LU\otimes M\|\limsup_{t\to\infty}\|\zeta(t)\|\\ \le&\|LU\|\|M\|\gamma_\zeta\limsup_{t\to\infty}\|\phi(t)\|.\end{aligned}$$

Finally, (34) can be put in the following compact form

$$\chi=-(L\otimes M)\sigma+(I_n\otimes M)\phi, \tag{49}$$

which gives

$$\begin{aligned}&\limsup_{t\to\infty}\|\chi(t)\|\\ \le&\|LU\|\|M\|\gamma_\zeta\limsup_{t\to\infty}\|\phi(t)\|+\|I_n\otimes M\|\limsup_{t\to\infty}\|\phi(t)\|\\ =&\|M\|(\|LU\|\gamma_\zeta+1)\limsup_{t\to\infty}\|\phi(t)\|.\end{aligned}$$

The proof is thus complete for $\gamma_\chi = \|M\|(\|LU\|\gamma_\zeta + 1)$. □

Remark 4.1: Under Assumption 1, let $\lambda_i,\ i = 2, \cdots n$, be the eigenvalues of H that have positive real parts. Under Assumption 2, let $G = G^\mathsf{T} > 0$ be the solution to the following algebraic Riccati equation

$$S^\mathsf{T}G + GS - \lambda^* GBB^\mathsf{T}G + \epsilon I = 0 \tag{50}$$

for some $0 < \lambda^* \leq \min_{i=2,\cdots N} \Re\{\lambda_i\}$ and $\epsilon > 0$. Let the controller gain matrix be $M = B^\mathsf{T}G/2$. Then, all the eigenvalues of $S - \lambda_i BM$ have strictly negative real parts and hence A_ζ in (39) is Hurwitz.

Remark 4.2: The concept of perturbed consensus was originally proposed in [36] to deal with the synchronization of heterogeneous nonlinear MASs using output communication, where the perturbation represents some trajectory regulation error. The technical novelty in this paper is multifold. On one hand, perturbed consensus is formulated in [36] in terms of a constant gain from a certain regulation error to ζ representing the consensus error. In Lemma 4.1, to facilitate the subsequent analysis of the overall system, perturbed consensus is formulated in terms of a different gain from the perturbation ϕ to χ as in (40). On the other hand, in solving the overall synchronization problem, the perturbed consensus technique in Lemma 4.1 must be integrated with the frequency observers, resulting in new challenging issues such as boundedness of the overall system states and satisfaction of a certain small-gain condition, which are not encountered in [36]. These issues will be addressed in the next section.

V. Synchronization of a Frequency Modulated MAS

With the frequency observers and the perturbed consensus controllers proposed in the previous two sections, it is ready to obtain the synchronization of a frequency modulated MAS using a small-gain argument. The result is stated in the following theorem.

Theorem 5.1: Consider the dynamics (1)*, the controller* (6)*, and the observer* (8)*, with a constant $\omega_c > 0$, under Assumptions 1 and 2. Suppose the frequency modulated signal $x(t)$ is bounded, i.e., $\underline{\alpha} \leq \|x(t)\| \leq \bar{\alpha}, \forall t \geq 0$, for some constants $\underline{\alpha}, \bar{\alpha} > 0$. Let M be selected such that A_ζ in* (39) *is Hurwitz and γ_ζ defined as* (48)*. Pick any*

$$0 < \gamma < \frac{1}{\|A\|\|M\|(\|LU\|\gamma_\zeta + 1)}. \tag{51}$$

If there exist matrices K_o and $P = P^\mathsf{T} > 0$ satisfying (11) *for $\gamma_o = \min\{\gamma/8, \gamma/\sqrt{8n}\}$, then, given any constants $b_\zeta, b_o > 0$, there exist control functions μ and κ such that synchronization is achieved in the sense of* (3) *for any initial state of the closed-loop system satisfying*

$$\begin{aligned} &\hat{x}_j^i(0) = x_j(0) \\ &\|(W \otimes I_p)\sigma(0)\| \leq b_\zeta \\ &\|\hat{\sigma}_j^i(0) - \sigma_j(0)\| \leq b_o,\ j \in \mathcal{N}_i,\ i \in \mathcal{V}. \end{aligned} \tag{52}$$

Proof: Lemmas 3.1 and 4.1 are the main tools used in this proof. Lemma 3.1 is valid under the condition of $\|\chi_i(t)\| \leq b_\chi,\ \forall t \geq 0$, for a constant b_χ; and Lemma 4.1 is valid under the condition that $\phi(t)$ is bounded. These two conditions do not hold separately, but they can be proved simultaneously for the closed-loop system in Step 1. Then, the two lemmas are applied to complete the proof using a small-gain argument in Step 2.

Step 1: For the matrix Q in (41), we first define two quantities

$$\begin{aligned} \pi_i^a =& \|L_iU\|\|M\|\sqrt{\varpi(Q)}b_\zeta \\ &+ (\|L_iU\|\|M\|\|A\mathbf{1}\|\gamma_\zeta + \|M\|\|A_i\mathbf{1}\|) \\ &\times (\sqrt{\varpi(P)}b_o + b_x b_K) > 0 \end{aligned}$$

and

$$\pi_i^b = 1 - (\|L_iU\|\|M\|\|A\mathbf{1}\|\gamma_\zeta + \|M\|\|A_i\mathbf{1}\|)\sqrt{8}\|PB\|\sqrt{\varpi(P)},$$

where b_x and b_K are defined in (19) and (20), L_i and A_i are the i-th rows of L and A, respectively.

By (11), one has

$$\sqrt{8n}\|PB\|\sqrt{\varpi(P)} < \gamma. \tag{53}$$

Noting $\|A\mathbf{1}\| \leq \sqrt{n}\|A\|$ and using (51) and (53), one has

$$\begin{aligned} &(\|L_iU\|\|M\|\|A\mathbf{1}\|\gamma_\zeta + \|M\|\|A_i\mathbf{1}\|)\sqrt{8}\|PB\|\sqrt{\varpi(P)} \\ <&\|A\mathbf{1}\|\|M\|(\|LU\|\gamma_\zeta + 1)\sqrt{8}\|PB\|\sqrt{\varpi(P)} \\ <&\|A\|\|M\|(\|LU\|\gamma_\zeta + 1)\sqrt{8n}\|PB\|\sqrt{\varpi(P)} < 1 \end{aligned}$$

and hence $\pi_i^b > 0$. Now, it is ready to pick

$$b_\chi > \frac{\pi_i^a}{\pi_i^b} > 0$$

and hence

$$b_\sigma = \sqrt{\varpi(P)b_o^2 + 8\|PB\|^2 b_\chi^2 \varpi(P)} + b_x b_K.$$

Next, we will prove that the signals $\phi(t)$ and $\chi_i(t)$ are bounded. First, it is noted that

$$\|\tilde{\sigma}_j^i(0)\| \leq b_o < b_\sigma.$$

Assume there exists a finite time $T > 0$ such that

$$\|\tilde{\sigma}_j^i(t)\| < b_\sigma,\ \forall t < T$$

and

$$\|\tilde{\sigma}_j^i(T)\| = b_\sigma. \tag{54}$$

A contradiction is derived below.

By the assumption, one has

$$\|\phi_i(t)\| \leq \sum_{j \in \mathcal{N}_i} a_{ij}\|\tilde{\sigma}_j^i(t)\| \leq \sum_{j \in \mathcal{N}_i} a_{ij} b_\sigma = \|A_i\mathbf{1}\|b_\sigma \tag{55}$$

and hence

$$\|\phi(t)\| \leq \|A\mathbf{1}\|b_\sigma, \tag{56}$$

which shows that $\phi(t)$ is bounded for $t \in [0, T]$.

Using (45) and (46) gives

$$\dot{V}(\zeta) \leq -\frac{V(\zeta)}{\lambda_{\max}(Q)} + \|Q(W \otimes BM)\|^2\|\phi\|^2.$$

As a result, for $t \in [0, T]$,

$$V(\zeta(t)) \leq V(\zeta(0)) + \|Q(W \otimes BM)\|^2\|A\mathbf{1}\|^2 b_\sigma^2 \lambda_{\max}(Q)$$

and

$$\begin{aligned} \|\zeta(t)\|^2 \leq& \frac{\lambda_{\max}(Q)\|\zeta(0)\|^2}{\lambda_{\min}(Q)} \\ &+ \|Q(W \otimes BM)\|^2\|A\mathbf{1}\|^2 b_\sigma^2 \frac{\lambda_{\max}(Q)}{\lambda_{\min}(Q)} \\ \leq& \varpi(Q)\|\zeta(0)\|^2 + \|A\mathbf{1}\|^2 b_\sigma^2 \gamma_\zeta^2. \end{aligned}$$

Then, we use the facts

$$(L_i \otimes I_p)\sigma = (L_iT^{-1} \otimes I_p)\begin{bmatrix} \bar{\sigma} \\ \zeta \end{bmatrix} = (L_iU \otimes I_p)\zeta$$

and

$$\chi_i = -(L_i \otimes M)\sigma + M\phi_i, \tag{57}$$

and have the following calculation, for $t \in [0, T]$,

$$\begin{aligned}\|\chi_i(t)\| \leq & \|(L_i \otimes M)\sigma(t)\| + \|M\|\|\phi_i(t)\| \\ \leq & \|L_i U \otimes M\|\|\zeta(t)\| + \|M\|\|\phi_i(t)\| \\ \leq & \|L_i U\|\|M\|\sqrt{\varpi(Q)\|\zeta(0)\|^2 + \|A\mathbf{1}\|^2 b_\sigma^2 \gamma_\zeta^2} \\ & + \|M\|\|A_i\mathbf{1}\|b_\sigma \\ \leq & \|L_i U\|\|M\|\sqrt{\varpi(Q)}b_\zeta \\ & + (\|L_i U\|\|M\|\|A\mathbf{1}\|\gamma_\zeta + \|M\|\|A_i\mathbf{1}\|)b_\sigma.\end{aligned}$$

Hence, we have the calculation

$$\begin{aligned}\|\chi_i(t)\| \leq & \|L_i U\|\|M\|\sqrt{\varpi(Q)}b_\zeta \\ & + (\|L_i U\|\|M\|\|A\mathbf{1}\|\gamma_\zeta + \|M\|\|A_i\mathbf{1}\|) \\ & (\sqrt{\varpi(P)b_o^2 + 8\|PB\|^2 b_\chi^2 \varpi(P)} + b_x b_K) \\ \leq & \|L_i U\|\|M\|\sqrt{\varpi(Q)}b_\zeta \\ & + (\|L_i U\|\|M\|\|A\mathbf{1}\|\gamma_\zeta + \|M\|\|A_i\mathbf{1}\|) \\ & (\sqrt{\varpi(P)}b_o + \sqrt{8}\|PB\|\sqrt{\varpi(P)}b_\chi + b_x b_K) \\ = & \pi_i^a + (1 - \pi_i^b)b_\chi < b_\chi.\end{aligned}$$

Denote $\bar{b}_\chi = \max_{i=1,\cdots,n}\{\pi_i^a + (1 - \pi_i^b)b_\chi\} < b_\chi$. One has

$$\|\chi_i(t)\| \leq \bar{b}_\chi,\ \forall t \in [0, T].$$

Using the similar development of (28) gives

$$\|\nu(t)\|^2 \leq \varpi(P)b_o^2 + 8\|PB\|^2 \bar{b}_\chi^2 \varpi(P). \tag{58}$$

Moreover, using (20) and (24) gives

$$\begin{aligned}\|\tilde{\sigma}_j^i(t)\| \leq & \|\nu(t)\| + \|K(\hat{x}(t))\tilde{x}(t)\| \\ \leq & \sqrt{\varpi(P)b_o^2 + 8\|PB\|^2 \bar{b}_\chi^2 \varpi(P)} + b_x b_K < b_\sigma,\end{aligned}$$

for $t \in [0, T]$. It contradicts with the assumption (54). Using the proof by contradiction, one has

$$\|\tilde{\sigma}_j^i(t)\| < b_\sigma,\ \|\phi(t)\| \leq \|A\mathbf{1}\|b_\sigma,\ \|\chi_i(t)\| \leq b_\chi,\ \forall t \geq 0. \tag{59}$$

Step 2: It is ready to apply Lemmas 3.1 and 4.1 to complete the proof using a small-gain argument. On one hand, by Lemma 3.1,

$$\limsup_{t\to\infty} \|\tilde{\sigma}_j^i(t)\| \leq \gamma \limsup_{t\to\infty} \|\chi_j(t)\|,\ j \in \mathcal{N}_i.$$

For $\phi_i = \sum_{j\in\mathcal{N}_i} a_{ij}\tilde{\sigma}_j^i$, one has

$$\limsup_{t\to\infty} \|\phi_i(t)\| \leq \gamma \sum_{j\in\mathcal{N}_i} a_{ij} \limsup_{t\to\infty} \|\chi_j(t)\|$$

and hence

$$\limsup_{t\to\infty} \|\phi(t)\| \leq \gamma\|A\| \limsup_{t\to\infty} \|\chi(t)\|. \tag{60}$$

On the other hand, by Lemma 4.1,

$$\limsup_{t\to\infty} \|\chi(t)\| \leq \gamma_\chi \limsup_{t\to\infty} \|\phi(t)\| \tag{61}$$

for $\gamma_\chi = \|M\|(\|LU\|\gamma_\zeta + 1)$ that satisfies the small-gain condition $\gamma\|A\|\gamma_\chi < 1$. Putting (60) and (61) together gives

$$\limsup_{t\to\infty} \|\phi(t)\| \leq \gamma\|A\|\gamma_\chi \limsup_{t\to\infty} \|\phi(t)\|. \tag{62}$$

It concludes the property

$$\lim_{t\to\infty} \|\phi(t)\| = 0.$$

Using the same approach also concludes

$$\lim_{t\to\infty} \|\chi(t)\| = 0.$$

Finally, by (47), one has

$$\lim_{t\to\infty} \|\zeta(t)\| = 0$$

and hence

$$\lim_{t\to\infty} \|\sigma(t) - (\mathbf{1} \otimes I_p)\bar{\sigma}(t)\| = \lim_{t\to\infty} \|(U \otimes I_p)\zeta(t)\| = 0,$$

which implies (3). The proof is thus completed. □

Remark 5.1: The functions μ and κ used in the observer (8) can be explicitly designed according to Lemma 3.1. It is seen in the proof of Lemma 3.1 that these functions depend on the function f and the parameters S, E, B, α, and b_χ. It is also seen from the proof of Theorem 5.1 that b_χ further depends on L, b_ζ, and b_o. Therefore, the two functions μ and κ are uniform for all the agents as shown in (8). As the constants b_ζ and b_o to characterize the initial states of the closed-loop system can be arbitrarily selected, the synchronization problem in Theorem 5.1 is solved in a semi-global sense. In this theorem, the existence of K_o and $P = P^\mathsf{T} > 0$ satisfying the first Lyapunov equation of (11) is always guaranteed when (S, E) is observable. However, the second inequality of (11) is more restrictive, which is needed for a sufficiently small γ_o to ensure the small-gain condition. A special case is given in Corollary 3.1, but the general solvability conditions deserve more investigation in the future research.

Remark 5.2: The full state of agent i is (σ_i, x_i) in the dynamics (1), where x_i is accessible by the neighboring agents via network but σ_i is not. Synchronization in terms of the full state trajectories $(\sigma_i(t), x_i(t))$ obviously includes synchronization of $\sigma_i(t)$ in the sense of (3). It is worth mentioning that the mechanism of frequency synchronization developed in this paper does not follow the traditional synchronization approach based on full state trajectories. In particular, the difference between the trajectories of two agents does not always approach zero, that is, $\lim_{t\to\infty} \|x_i(t) - x_j(t)\|$ does not necessarily exist or is not equal to zero, even when (3) is guaranteed.

VI. Numerical Examples

Two examples are used to demonstrate the effectiveness of the approach developed in this paper. The numerical simulation run in MATLAB® with the ordinary differential equation (ODE) solver ode23. The relative and absolute error tolerances are 10^{-4} and 10^{-8}, respectively. The noise in the simulation is generated by the function rand.

In the first example, we consider of a network of $n = 6$ frequency modulated sinusoidal oscillators of the form (1) with

$$S = \begin{bmatrix} 0 & 0.1 \\ -0.1 & 0 \end{bmatrix},\ B = \begin{bmatrix} 1 \\ 1 \end{bmatrix},\ E = \begin{bmatrix} 4.5 & 0 \end{bmatrix}$$

and

$$f(x_i) = \begin{bmatrix} 0 & 1 \\ -1 & 0 \end{bmatrix} x_i,\ f_o(x_i) = 0,\ \omega_c = 3.$$

In this example, the modulated signals $x_i(t)$ are frequency-varying sinusoids. The target is to synchronize the frequencies of the signals generated by the oscillators, not the instantaneous values of the signals. The network topology is illustrated in Fig. 2.

The function

$$K(\hat{x}) = K_o \frac{\hat{x}^\mathsf{T}}{\|\hat{x}\|^2} \begin{bmatrix} 0 & -1 \\ 1 & 0 \end{bmatrix},\ K_o = \begin{bmatrix} 1.80 \\ 1.76 \end{bmatrix},$$

This article has been accepted for publication in IEEE Transactions on Automatic Control. This is the author's version which has not been fully edited and content may change prior to final publication. Citation information: DOI 10.1109/TAC.2022.3197125

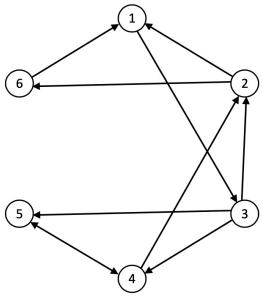

Fig. 2. Illustration of the network topology of six oscillators (agents) where the weight associated with each edge (arrowed line) is positive.

with

$$K'(x,\hat{x},\hat{\sigma}) = K_o \left(\frac{I_2 - 2f(\hat{x})f^{\mathsf{T}}(\hat{x})}{\|\hat{x}\|^2} \times \begin{bmatrix} 0 & 1 \\ -1 & 0 \end{bmatrix} (f(x)\hat{\omega} + \kappa(x,\hat{x})) \right)^{\mathsf{T}},$$

is used to construct the functions μ and κ of the frequency observers. The parameter $\beta = 10$ is used for the simulation. It is noted that a higher value of β gives faster convergence of the frequency observers. For $a_{ij} = 1,\ \forall\,(i,j) \in \mathcal{E}$, the gain matrix $M = 0.01 \begin{bmatrix} 1 & 0.5 \end{bmatrix}$, representing weak coupling among the oscillators, is used in the controller. Under the observer/controller proposed in the paper, the synchronization performance of the oscillators is discussed below. In the figures, we only demonstrate the trajectories of three oscillators, denoted as OSC 1, OSC 3, and OSC 5, corresponding to the nodes 1, 3, and 5 in Fig. 2, respectively. The other three oscillators have similar profiles and thus omitted.

The profile of the frequency modulated signals $x_i(t)$ (only the first component $x_{i1}(t)$ for concise presentation) is shown in Fig. 3. Frequency synchronization can be observed in this figure as expected, but synchronization of the signals in oscillation phase or amplitude is not needed. Frequency synchronization can also be exhibited in Fig. 4 in an explicit illustration. It is noted that the frequency $\omega_i(t)$ in this figure is not directly measured or transmitted via the network. The effectiveness of the proposed frequency observer is verified in Fig. 5. According to the topology, the frequency of OSC 1 is observed by agent 3, that of OSC 3 by agents 2, 4, 5, separately, and that of OSC 5 by agent 4. The convergence of the observed frequencies (dashed curves) to the real values (solid curves) can be achieved by all the observers .

Next, we consider the second example of a network of Hindmarsh-Rose oscillators of the dynamics (2) with the parameters $c_1 = 3, c_2 = 1, c_3 = 5, c_4 = 1, c_5 = 0.005, c_6 = 4, c_7 = 1.5$, and $c_I = 2$. The other parameters in (1) are $\omega_c = 0.9$ and

$$S = \begin{bmatrix} 0 & 0.005\pi \\ -0.005\pi & 0 \end{bmatrix},\ B = \begin{bmatrix} 1 \\ 1 \end{bmatrix},\ E = \begin{bmatrix} 0.4 & 0 \end{bmatrix}.$$

The network topology is the same one in Fig. 2. The non-sinusoidal signals $x_i(t)$ of this class of oscillators consist of bursts and spikes of varying firing rates. The synchronization target is not the instantaneous signals but their firing rates.

The results discussed in the first example can be observed in this example as well. As a comparison, the membrane potentials of the individual oscillators without synchronization control, i.e., $\chi_i = 0$, are plotted in Fig. 6. With the synchronization controller proposed in this paper, frequency synchronization of membrane potentials is plotted in Fig. 7 and synchronization of firing rates of spikes in

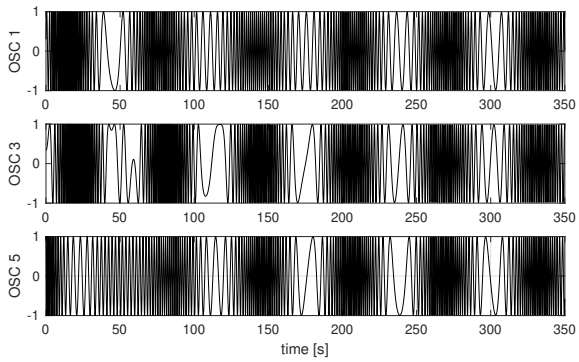

Fig. 3. Profile of the frequency modulated signals $x_{i1}(t)$, the first element of the state vector $x_i(t)$ of sinusoidal oscillators, for $i = 1, 3, 5$.

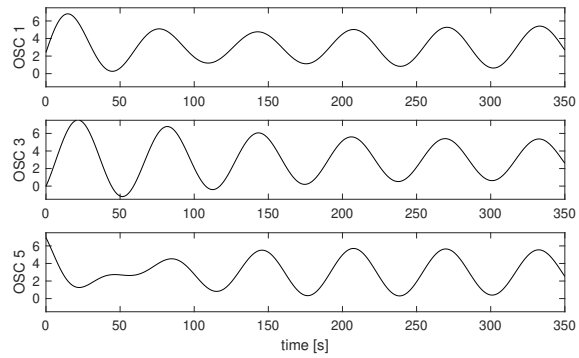

Fig. 4. Profile of the frequencies $\omega_i(t)$ of sinusoidal oscillators for $i = 1, 3, 5$.

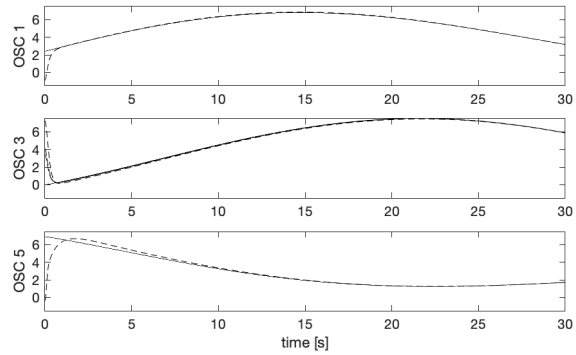

Fig. 5. Profile of the observed frequencies $\hat{\omega}_j^i(t)$, $j \in \mathcal{N}_i$ (dashed curves) vs the real frequencies $\omega_j(t)$ (solid curves) of sinusoidal oscillators, for $j = 1, 3, 5$.

Fig. 8. Once synchronized, the firing rates of spikes are generally less than those of individual oscillators because the variations of the firing rates are averaged. It is also noted that the signals in terms of the instantaneous values are not necessarily synchronized. The convergence of the observed firing rates to the real values is shown in Fig. 9. The results well demonstrate the similar phenomenon observed in real neural circuits.

Finally, we examine the robustness of synchronization of frequency modulated oscillators with respect to noise. It is worth mentioning that the frequency observer (10) has yet deliberately addressed its robustness, because the design of the observer, in particular, the function $\kappa(x,\hat{x})$, relies on the precise knowledge of the model (9) and the precise measurement of the state x. Therefore, the robustness of the approach developed in this paper deserves deeper theoretical

This article has been accepted for publication in IEEE Transactions on Automatic Control. This is the author's version which has not been fully edited and content may change prior to final publication. Citation information: DOI 10.1109/TAC.2022.3197125

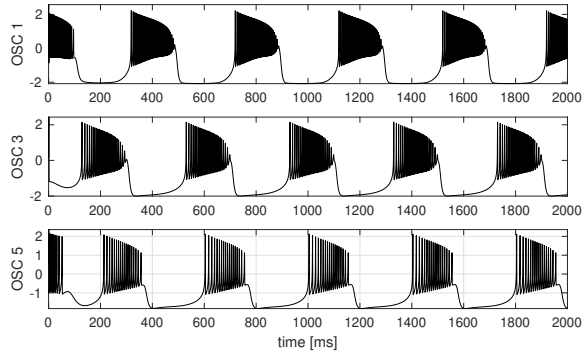

Fig. 6. Profile of the membrane potentials $v_i(t)$ of individual Hindmarsh-Rose oscillators without synchronization for $i = 1, 3, 5$.

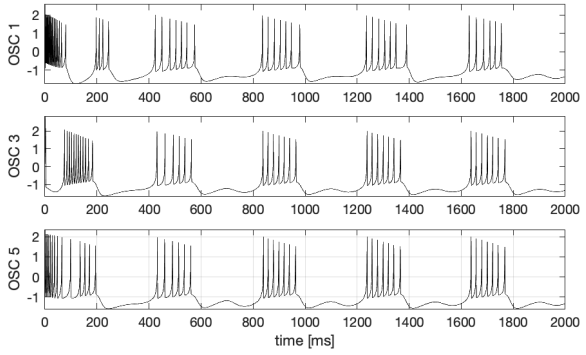

Fig. 7. Profile of the membrane potentials $v_i(t)$ of Hindmarsh-Rose oscillators for $i = 1, 3, 5$.

analysis. Nevertheless, it is interesting to numerically observe the robustness of the present design in the two examples. The observation is depicted in Figs. 10 and 11 in terms of the synchronization error $\omega_1(t) - \omega_3(t)$ for the above two examples, respectively.

The top graph of Fig. 10 shows a perfect synchronization behavior in the first example without any noticeable error in the scale of ± 0.01. The middle graph shows the result for the unmodulated controller (5) with transmission noise, i.e,

$$\chi_i = -M \sum_{j \in \mathcal{N}_i} a_{ij}(\sigma_i - \sigma_j - \mathrm{n}_j^i),\ i \in \mathcal{V},$$

where the level of noise n_j^i on σ_j transmitted from j to i is $\pm 1\%$ of the magnitude of the transmitted signal. In this case, the synchronization error induced by the noise can be obviously observed. Then, we apply the same level of noise on the frequency modulated controller (8), i.e.,

$$\begin{aligned}
\dot{\hat{\sigma}}_j^i &= S\hat{\sigma}_j^i + \mu(x_j + \mathrm{n}_j^i, \hat{x}_j^i, \hat{\sigma}_j^i) \\
\hat{\omega}_j^i &= E\hat{\sigma}_j^i + \omega_c \\
\dot{\hat{x}}_j^i &= f(\hat{x}_j^i)\hat{\omega}_j^i + f_o(x_j + \mathrm{n}_j^i) + \kappa(x_j + \mathrm{n}_j^i, \hat{x}_j^i),\ j \in \mathcal{N}_i,\ i \in \mathcal{V}.
\end{aligned}$$

The result in the bottom graph exhibits that the synchronization error using frequency modulation is significantly less than that in the unmodulated case. The error is noticeable with more details when it is amplified to the scale of 10^{-4}. The comparison in Fig. 10 exhibits the robustness of the frequency modulated MASs in mitigating the influence of network noise.

Robustness with respect to external noise to oscillator dynamics is examined in Fig. 11 for the second example. Similarly, the top graph shows a perfect synchronization behavior without any noticeable error in the scale of 10^{-3}. The middle graph shows the result for the unmodulated controller (5) based on the dynamics

$$\dot{\sigma}_i = S\sigma_i + B\chi_i + \mathrm{n}_i,\ i \in \mathcal{V}, \tag{63}$$

subject to the external noise n_i. In this case, the synchronization error induced by the noise can be obviously observed. Then, we apply the frequency modulated controller (8) based on the dynamics

$$\dot{x}_i = f(x_i)\omega_i + f_o(x_i) + \mathrm{n}_i,\ i \in \mathcal{V}, \tag{64}$$

subject to the external noise n_i of the same level of magnitude. The result in the bottom graph exhibits that the synchronization error using frequency modulation is significantly less than that in the unmodulated case. The error is noticeable with more details when it is amplified to the scale of 10^{-5}. The comparison in Fig. 11 exhibits the robustness of the frequency modulated MASs in mitigating the influence of external noise to oscillator dynamics.

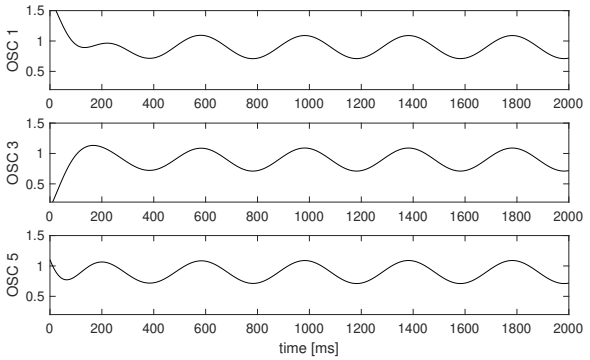

Fig. 8. Profile of the firing rates $\omega_i(t)$ of Hindmarsh-Rose oscillators for $i = 1, 3, 5$.

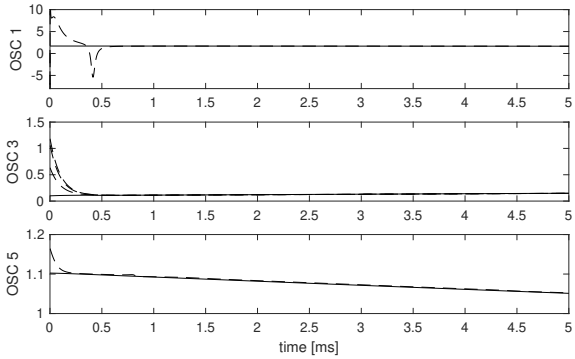

Fig. 9. Profile of the observed firing rates $\hat{\omega}_j^i(t)$, $j \in \mathcal{N}_i$ (dashed curves) vs the real firing rates $\omega_j(t)$ (solid curves) of Hindmarsh-Rose oscillators for $j = 1, 3, 5$.

VII. Conclusion

In this paper, we have established a framework for the synchronization of frequency modulated multi-agent systems for the first time. The framework includes a frequency observer subject to an external input and a distributed synchronization controller based on the observer using the small-gain argument. We have verified the effectiveness of the design using rigorous theoretical proofs and extensive numerical simulation. It would be interesting to further extend the framework to study more complicated models, especially from biological neural networks. The research for unmodulated multi-agent systems has experienced rapid development in the recent decade, which can be further developed for frequency modulated multi-agent systems using the framework in this paper. The robust synchronization mechanism using frequency modulated signals is

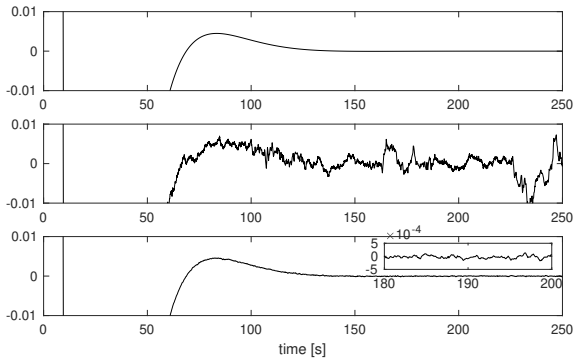

Fig. 10. Profile of the synchronization error $\omega_1(t) - \omega_3(t)$ of sinusoidal oscillators in three cases. Top graph: noise free; middle graph: unmodulated synchronization with noise; and bottom graph: frequency modulated synchronization with noise.

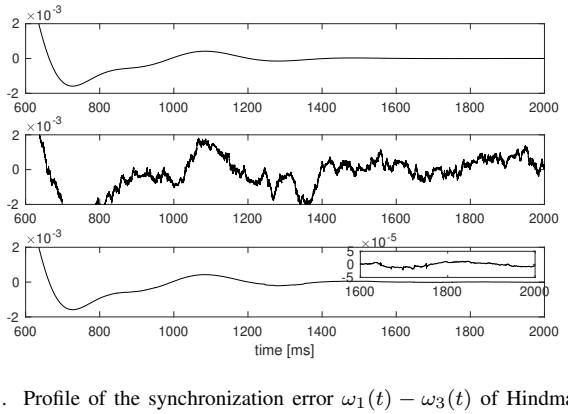

Fig. 11. Profile of the synchronization error $\omega_1(t) - \omega_3(t)$ of Hindmarsh-Rose oscillators in three cases for the second example. Top graph: noise free; middle graph: unmodulated synchronization with noise; and bottom graph: frequency modulated synchronization with noise.

an interesting topic for future research, and it has the potential of revealing the similar phenomenon in biological systems and gaining a deep understanding of how neuronal circuits generate highly robust and adaptive oscillatory behaviors in animal locomotion. It is expected that the research along this direction is also beneficial for building artificial frequency modulated multi-agent systems to pursue more complex dynamical regimes, such as multi-clustering and formation, with more engineering applications.

REFERENCES

[1] W. Gerstner, A. K. Kreiter, H. Markram, and A. V. Herz, "Neural codes: firing rates and beyond," *Proceedings of the National Academy of Sciences*, vol. 94, no. 24, pp. 12 740–12 741, 1997.

[2] J. M. Newcomb, A. Sakurai, J. L. Lillvis, C. A. Gunaratne, and P. S. Katz, "Homology and homoplasy of swimming behaviors and neural circuits in the nudipleura (mollusca, gastropoda, opisthobranchia)," *Proceedings of the National Academy of Sciences*, vol. 109, no. Supplement 1, pp. 10 669–10 676, 2012.

[3] J. Saeedi and K. Faez, "Synthetic aperture radar imaging using nonlinear frequency modulation signal," *IEEE Transactions on Aerospace and Electronic Systems*, vol. 52, no. 1, pp. 99–110, 2016.

[4] H.-J. Choi and J.-H. Jung, "Enhanced power line communication strategy for DC microgrids using switching frequency modulation of power converters," *IEEE Transactions on Power Electronics*, vol. 32, no. 6, pp. 4140–4144, 2017.

[5] Z. Wang, Y. Wang, and L. Xu, "Parameter estimation of hybrid linear frequency modulation-sinusoidal frequency modulation signal," *IEEE Signal Processing Letters*, vol. 24, no. 8, pp. 1238–1241, 2017.

[6] M. A. Lewis, F. Tenore, and R. Etienne-Cummings, "CPG design using inhibitory networks," in *Proceedings of the 2005 IEEE International Conference on Robotics and Automation*. IEEE, 2005, pp. 3682–3687.

[7] A. J. Ijspeert, A. Crespi, D. Ryczko, and J.-M. Cabelguen, "From swimming to walking with a salamander robot driven by a spinal cord model," *Science*, vol. 315, no. 5817, pp. 1416–1420, 2007.

[8] A. Spaeth, M. Tebyani, D. Haussler, and M. Teodorescu, "Spiking neural state machine for gait frequency entrainment in a flexible modular robot," *PloS One*, vol. 15, no. 10, p. e0240267, 2020.

[9] I. Y. Tyukin, D. V. Prokhorov, and C. van Leeuwen, "Adaptation and parameter estimation in systems with unstable target dynamics and nonlinear parametrization," *IEEE transactions on automatic control*, vol. 52, no. 9, pp. 1543–1559, 2007.

[10] Z. Chen, "A novel adaptive control approach for nonlinearly parameterized systems," *International Journal of Adaptive Control and Signal Processing*, vol. 29, no. 1, pp. 81–98, 2015.

[11] E. O. Olivares, E. J. Izquierdo, and R. D. Beer, "Potential role of a ventral nerve cord central pattern generator in forward and backward locomotion in caenorhabditis elegans," *Network Neuroscience*, vol. 2, no. 3, pp. 323–343, 2018.

[12] L. Hachoumi and K. T. Sillar, "Developmental stage-dependent switching in the neuromodulation of vertebrate locomotor central pattern generator networks," *Developmental Neurobiology*, vol. 80, no. 1-2, pp. 42–57, 2020.

[13] W. Friesen and C. Hocker, "Functional analyses of the leech swim oscillator," *J. Neurophysiol.*, vol. 86, pp. 824–835, 2001.

[14] Z. Chen, M. Zheng, W. O. Friesen, and T. Iwasaki, "Multivariable harmonic balance analysis of neuronal oscillator for leech swimming," *Journal of Computational Neuroscience*, vol. 25, pp. 583–606, 2008.

[15] T. Iwasaki, J. Chen, and W. O. Friesen, "Biological clockwork underlying adaptive rhythmic movements," *Proceedings of the National Academy of Sciences*, vol. 111, no. 3, pp. 978–983, 2014.

[16] L. Scardovi and R. Sepulchre, "Synchronization in networks of identical linear systems," *Automatica*, vol. 45, no. 11, pp. 2557–2562, 2009.

[17] S. E. Tuna, "LQR-based coupling gain for synchronization of linear systems," *arXiv preprint arXiv:0801.3390*, 2008.

[18] J. Seo, H. Shim, and J. Back, "Consensus of high-order linear systems using dynamic output feedback compensator: Low gain approach," *Automatica*, vol. 45, no. 11, pp. 2659–2664, 2009.

[19] S. E. Tuna, "Synchronizing linear systems via partial-state coupling," *Automatica*, vol. 44, no. 8, pp. 2179–2184, 2008.

[20] K. You and L. Xie, "Network topology and communication data rate for consensusability of discrete-time multi-agent systems," *IEEE Transactions on Automatic Control*, vol. 56, no. 10, pp. 2262–2275, 2011.

[21] A. A. Stoorvogel, A. Saberi, M. Zhang, and Z. Liu, "Solvability conditions and design for synchronization of discrete-time multiagent systems," *International Journal of Robust and Nonlinear Control*, vol. 28, no. 4, pp. 1381–1401, 2018.

[22] S. Knorn, Z. Chen, and R. H. Middleton, "Overview: Collective control of multiagent systems," *IEEE Transactions on Control of Network Systems*, vol. 3, no. 4, pp. 334–347, Dec 2016.

[23] H. Modares, B. Kiumarsi, F. L. Lewis, F. Ferrese, and A. Davoudi, "Resilient and robust synchronization of multiagent systems under attacks on sensors and actuators," *IEEE Transactions on Cybernetics*, vol. 50, no. 3, pp. 1240–1250, 2019.

[24] G. Jing and L. Wang, "Multiagent flocking with angle-based formation shape control," *IEEE Transactions on Automatic Control*, vol. 65, no. 2, pp. 817–823, 2019.

[25] P. Wieland, R. Sepulchre, and F. Allgöwer, "An internal model principle is necessary and sufficient for linear output synchronization," *Automatica*, vol. 47, no. 5, pp. 1068–1074, 2011.

[26] H. Kim, H. Shim, and J. H. Seo, "Output consensus of heterogeneous uncertain linear multi-agent systems," *IEEE Transactions on Automatic Control*, vol. 56, no. 1, pp. 200–206, 2011.

[27] T. Yang, A. Saberi, A. A. Stoorvogel, and H. F. Grip, "Output synchronization for heterogeneous networks of introspective right-invertible agents," *International Journal of Robust and Nonlinear Control*, vol. 24, no. 13, pp. 1821–1844, 2014.

[28] L. Zhu and Z. Chen, "Robust homogenization and consensus of nonlinear multi-agent systems," *Systems and Control Letters*, vol. 65, pp. 50–55, 2014.

[29] J. Lunze, "Synchronization of heterogeneous agents," *IEEE Transactions on Automatic Control*, vol. 57, no. 11, pp. 2885–2890, 2012.

[30] H. Grip, A. Saberi, and A. Stoorvogel, "On the existence of virtual exosystems for synchronized linear networks," *Automatica*, vol. 49, no. 10, pp. 3145–3148, 2013.

[31] L. Pecora and T. Carroll, "Synchronization in chaotic systems," *Physical Review Letters*, vol. 64, no. 8, p. 821, 1990.

[32] N. Chopra and M. Spong, "On exponential synchronization of Kuramoto oscillators," *IEEE Transactions on Automatic Control*, vol. 54, no. 2, pp. 353–357, 2009.

[33] H. Su, X. Wang, and Z. Lin, "Synchronization of coupled harmonic oscillators in a dynamic proximity network," *Automatica*, vol. 45, no. 10, pp. 2286–2291, 2009.

[34] A. Isidori, L. Marconi, and G. Casadei, "Robust output synchronization of a network of heterogeneous nonlinear agents via nonlinear regulation theory," *IEEE Transactions on Automatic Control*, vol. 59, no. 10, pp. 2680–2691, 2014.

[35] X. Chen and Z. Chen, "Robust perturbed output regulation and synchronization of nonlinear heterogeneous multiagents," *IEEE Transactions on Cybernetics*, vol. 46, no. 12, pp. 3111–3122, 2015.

[36] L. Zhu, Z. Chen, and R. Middleton, "A general framework for robust output synchronization of heterogeneous nonlinear networked systems," *IEEE Transactions on Automatic Control*, vol. 61, no. 8, pp. 2092–2107, 2016.

[37] Y. Su and J. Huang, "Cooperative global robust output regulation for nonlinear uncertain multi-agent systems in lower triangular form," *IEEE Transactions on Automatic Control*, vol. 60, no. 9, pp. 2378–2389, 2015.

[38] H. Cai, F. L. Lewis, G. Hu, and J. Huang, "The adaptive distributed observer approach to the cooperative output regulation of linear multi-agent systems," *Automatica*, vol. 75, pp. 299–305, 2017.

[39] J. Huang, "The cooperative output regulation problem of discrete-time linear multi-agent systems by the adaptive distributed observer," *IEEE Transactions on Automatic Control*, vol. 62, no. 4, pp. 1979–1984, 2017.

[40] Y. Yan and Z. Chen, "Cooperative output regulation of linear discrete-time time-delay multi-agent systems by adaptive distributed observers," *Neurocomputing*, vol. 331, pp. 33–39, 2019.

[41] E. Panteley, *A Stability-Theory Perspective to Synchronization of Heterogeneous Networks (Drsc Dissertation)*. University Paris Sud, Orsay, France, 2015.

[42] E. Panteley and A. Loría, "Synchronization and dynamic consensus of heterogeneous networked systems," *IEEE Transactions on Automatic Control*, vol. 62, no. 8, pp. 3758–3773, 2017.

[43] M. Maghenem, E. Panteley, and A. Loria, "Singular-perturbations-based analysis of synchronization in heterogeneous networks: A case-study," in *2016 IEEE 55th Conference on Decision and Control (CDC)*, 2016, pp. 2581–2586.

[44] E. Panteley, A. Loria, and A. El-Ati, "Practical dynamic consensus of Stuart-Landau oscillators over heterogeneous networks," *International Journal of Control*, vol. 93, no. 2, pp. 261–273, 2020.

[45] Y. Yan, Z. Chen, and R. Middleton, "Autonomous synchronization of heterogeneous multi-agent systems," *IEEE Transactions on Control of Network Systems*, vol. 8, no. 2, pp. 940–950, 2021.

[46] Z. Hu, Z. Chen, and H. T. Zhang, "Necessary and sufficient conditions for asymptotic decoupling of stable modes in LTV systems," *IEEE Transactions on Automatic Control*, vol. 66, no. 10, pp. 4546–4559, 2021.

[47] J. L. Hindmarsh and R. Rose, "A model of neuronal bursting using three coupled first order differential equations," *Proceedings of the Royal society of London. Series B. Biological sciences*, vol. 221, no. 1222, pp. 87–102, 1984.

[48] Z. Chen and J. Huang, *Stabilization and Regulation of Nonlinear Systems*. Springer, 2005.

[49] X.-H. Xia and W.-B. Gao, "Nonlinear observer design by observer error linearization," *SIAM Journal on Control and Optimization*, vol. 27, no. 1, pp. 199–216, 1989.

[50] M. Zeitz, "The extended Luenberger observer for nonlinear systems," *Systems and Control Letters*, vol. 9, no. 2, pp. 149–156, 1987.

[51] H. K. Khalil and L. Praly, "High-gain observers in nonlinear feedback control," *International Journal of Robust and Nonlinear Control*, vol. 24, no. 6, pp. 993–1015, 2014.

[52] D. Astolfi and L. Marconi, "A high-gain nonlinear observer with limited gain power," *IEEE Transactions on Automatic Control*, vol. 60, no. 11, pp. 3059–3064, 2015.

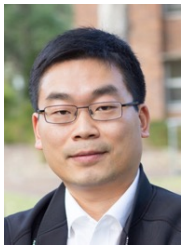

Zhiyong Chen received the B.E. degree in automation from the University of Science and Technology of China, Hefei, China, in 2000, and the M.Phil. and Ph.D. degrees in mechanical and automation engineering from the Chinese University of Hong Kong, in 2002 and 2005, respectively. He worked as a Research Associate at the University of Virginia, Charlottesville, VA, USA from 2005 to 2006. In 2006, he joined the University of Newcastle, Callaghan, NSW, Australia, where he is currently a Professor. He was also a Changjiang Chair Professor with Central South University, Changsha, China. His research interests include nonlinear systems and control, biological systems, and reinforcement learning. Dr. Chen is/was an Associate Editor of Automatica, IEEE Transactions on Automatic Control, IEEE Transactions on Neural Networks and Learning Systems, and IEEE Transactions on Cybernetics.